

BEAM-BEAM INTERACTION: LUMINOSITY, TAILS, AND NOISE*

JOHN T. SEEMAN

Stanford Linear Accelerator Center

Stanford University, Stanford, California 94305

Summary Observations of the beam-beam interaction at SPEAR, CESR, PETRA and PEP are discussed. They are sufficiently similar that a simple prescription can be formulated to describe the behavior of the luminosity as a function of current including the peak values. With this prescription the interpretation of various methods of increasing the luminosity, such as the reduction of the vertical betatron function, the increase of the horizontal beam size, and "mini-" and "micro-" beta projects, is straight-forward. Predictions for future storage rings can also be made. Finally, some observations of the consequences of reducing the vertical betatron function to near the value of the bunch length are discussed.

Standard Luminosity and Tune Shift Equations The luminosity L is given by^{1,2}

$$L = \frac{I^2}{4\pi k e^2 f \sigma_x^* \sigma_y^*} \quad (1)$$

where I is the current per beam, e the charge of the electron, f the revolution frequency, k the number of bunches per beam, and σ_x^* and σ_y^* the horizontal (x) and vertical (y) gaussian beam sizes at the crossing point. The beam-beam tune shift parameters are given by

$$\xi_y = \frac{I r_e \beta_y^*}{2\pi k e f (\sigma_x^* + \sigma_y^*) \sigma_y^* \gamma} \quad (2)$$

and

$$\xi_x = \frac{I r_e \beta_x^*}{2\pi k e f (\sigma_x^* + \sigma_y^*) \sigma_x^* \gamma} \quad (3)$$

where γ is the electron energy divided by its rest energy, $r_e = 2.82 \times 10^{-13}$ cm, and β_x^* and β_y^* are the horizontal and vertical betatron functions at the crossing point. Equations (1) and (2) can be combined to give

$$L = \frac{I \gamma \xi_y}{2e r_e \beta_y^*} \quad (4)$$

assuming $\sigma_x^* \gg \sigma_y^*$. The linear tune shift³ per crossing $\Delta\nu$ can be calculated from the tune shift parameter ξ .

$$\cos 2\pi(\nu_0 + \Delta\nu) = \cos 2\pi\nu_0 - 2\pi\xi \sin 2\pi\nu_0 \quad (5)$$

where ν_0 is the betatron tune per crossing. The betatron function at the crossing β is also shifted from the nominal value β_0 .

$$\beta \sin 2\pi(\nu_0 + \Delta\nu) = \beta_0 \sin 2\pi\nu_0 \quad (6)$$

Consequently, the betatron functions throughout the ring are affected as well as the radiation integrals.

Observations Several lattices for SPEAR, CESR, PETRA, and PEP used for high energy physics data taking and limited by the beam-beam interaction are compared here. The data for SPEAR came from Refs. 4 and 5, CESR Refs. 6, 7 and 8, PETRA Refs. 9 and 10, and PEP Refs. 11, 12 and 13. Some parameters for each machine are given in Table 1 and the measured luminosities as a function of current for those parameters

are shown in Fig. 1. The obvious feature is that, although at low currents the luminosity is proportional to the current squared as expected from Eq. (1), at high currents the luminosity deviates from that behavior and is not inconsistent with being proportional to current. If the luminosity is proportional to current, then from Eq. (4) the vertical tune shift parameter ξ_y must be constant. The calculated values of ξ_y as a function of current for these four lattices are also shown in Fig. 1. Indeed, ξ_y is nearly constant at high currents. Finally, if ξ_y is constant and the horizontal beam size does not change with current (as is measured), the vertical beam size must grow linearly with current.

Table 1. Parameters for SPEAR, CESR, PETRA and PEP

Parameter	SPEAR	CESR	PETRA	PEP
E_0 (GeV)	1.89	5.28	11.0	14.5
k	1	1	2	3
δ ($\times 10^{-5}$)	1.5	4.8	7.7	13.6
ν_x	5.28	9.39	25.19	21.25
ν_y	5.18	9.37	23.12	18.19
β_y^* (cm)	10	3.0	9	11
β_x^* (m)	1.2	1.25	1.3	3.0
η_x^* (m)	0	1.1	0	0
I_{max} (mA)	15.6	18	11.4	24.8
ξ_y max	0.039	0.020	0.024	0.046
ξ_x max	0.021	0.021	0.034	0.050
L_{max} [$\times 10^{30} \text{ cm}^{-2} \text{ sec}^{-1}$]	2.6	15	8	32.3

The vertical and horizontal cores of the beams can be measured with synchrotron radiation profile monitors using optical¹⁴ or x-ray¹⁵ wavelengths. Observations of the horizontal cores of the beams in each machine show little if any enlargement. Observations of the vertical cores of the beams show significant enlargement. For example, the data for the vertical core enlargement for the CESR lattice are shown in Fig. 2. The core is observed to increase linearly with current above the break in the L versus I curve. Similar observations have been obtained at SPEAR and PEP. These data substantiate the luminosity measurements.

The tails of the horizontal and vertical particle distributions of the beams during collisions can be measured using scrapers¹⁶ or probing fingers.¹⁷ Only scraper data are studied here as scrapers mimic fixed physical apertures. The positions of the scraper which reduces the beam lifetime to around two hours, about the shortest useful for the operation of a storage ring, are recorded. The vertical data as a function of current during collisions at SPEAR and CESR are shown in Fig. 2. Clearly for both machines, the vertical tails grow in proportion to the current. Thus, the vertical cores and tails of the beams have the same current dependence. Measurements of the horizontal tails show only small changes.

Another indication that the tails of the particle distributions are quite extended comes from the background noise in the experimental detectors. In Fig. 2 measurements of the noise versus current for SPEAR, CESR and PEP are shown. In all three cases the noise increases slowly with current, then rapidly near the peak values. The source of the noise is consistent with

*Work supported by the Department of Energy, contract DE-AC03-76SF00515.

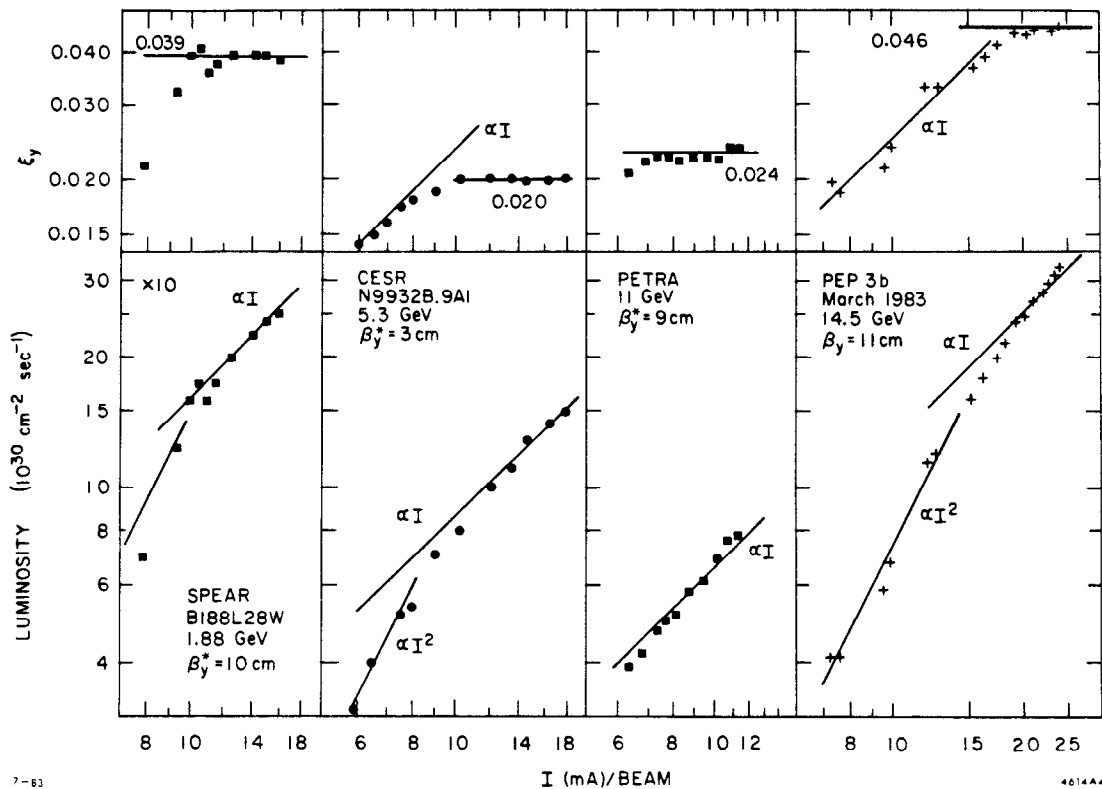


Fig. 1. Luminosity and vertical tune shift parameter versus beam current for SPEAR, CESR, PETRA and PEP.

hard particles. These observations can be explained by substantial tails of the beams exceeding the vertical acceptance.

A very instructive exercise is to compare the smallest vertical aperture in a storage ring to the enlarged core and tail sizes at that aperture. A schematic view of the quantities involved is shown in Fig. 3. The half-height of the tightest vertical aperture in the ring is denoted by y_A and is shown near the first interaction region (IR) quadrupole where it is most often located although need not be. The scraper setting translated to the location of the tightest aperture using the betatron functions is y_s . A translated vertical beam size as determined by the beam-beam interaction is y_σ . The ratios y_A/y_σ and y_s/y_A have been calculated for several lattices per machine at the peak currents and also at low currents. The results are listed in Table 2. Only lattices limited by the beam-beam interaction are included. The translated scraper settings correspond to two-hour lifetime positions. The effects on the betatron functions due to the tune shifts have been incorporated (small except for PEP). Three conclusions can be drawn. (1) Both the core and tails increase dramatically from low to high currents. (2) The scraper positions at the peak currents and luminosities are consistent with the physical apertures of the storage rings. (3) The ratio of the physical aperture to the translated maximum vertical beam size in all cases is very close to the value of twenty. The anomalous value for y_A/y_σ for the CESR lattice N992BC.9A1 results from a very low value of β_y^* (2.45 cm) and is discussed later.

Table 2. Comparison of the beam core and tails to the smallest vertical aperture at the maximum beam current and luminosity and at low currents.

Machine	Lattice (at maximum luminosity)	$\frac{y_A}{y_\sigma}$	$\frac{y_s}{y_A}$
SPEAR	TEM188/4A	22	0.83
SPEAR	TEM188/5	20	0.91
SPEAR	B188L28W	25	0.87
CESR	L3538.002	21	0.83
CESR	E99XX6.9A0	22	0.94
CESR	G99328.9A0	21	0.96
CESR	N9932B.9A1	24	0.92
CESR	N992BC.9A1	31	0.85
PETRA	7 GeV mini β	16	—
PETRA	11 GeV mini β	26	—
PEP	Spring 1981	17	—
PEP	Spring 1983	19	—
(at low current)			
SPEAR	B188L28W	40	0.27
CESR	N9932B.9A1	48	0.57
PETRA	11 GeV mini β	46	—
PEP	Spring 1983	28	—

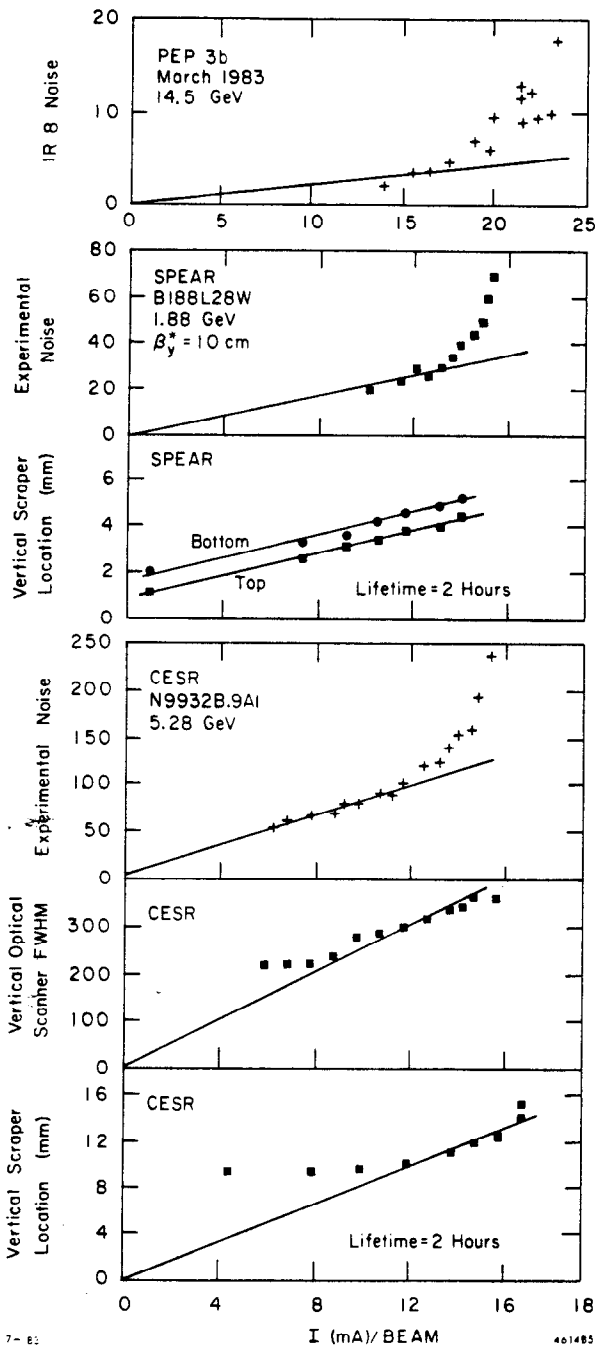


Fig. 2. Various measurements of the transverse beam size versus beam current at SPEAR, CESR and PEP.

Maximum Tune Shift Values Keil and Talman¹⁸ suggest that the proper parameter to compare the tune shifts between machines is the damping decrement δ , the transverse damping per collision.

$$\delta = \frac{1}{2kf\tau_y} \quad (7)$$

where τ_y is the transverse, say vertical, damping time. $\xi_{y \max}$ values for the four machines at various energies are plotted ver-

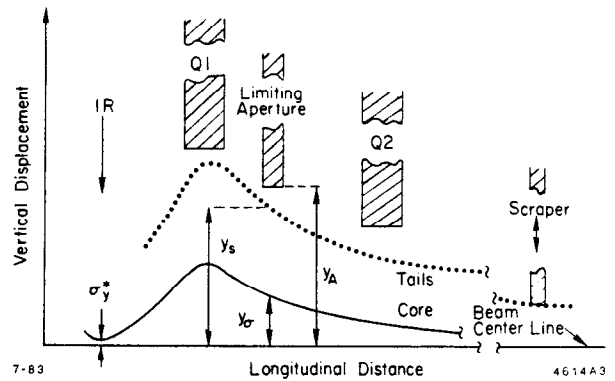


Fig. 3. Schematic view of the tightest vertical aperture, the translated scraper position, and the translated beam-beam determined core size.

sus δ in Fig. 4. The PEP point at high δ is a result of collisions with one bunch per beam.¹³ There is a marked rise in $\xi_{y \max}$ with δ . The linear tune shifts $\Delta\nu_{x \max}$ and $\Delta\nu_{y \max}$ can be calculated from Eq. (5). They are also plotted in Fig. 4. There is a strong correlation between $\Delta\nu_{y \max}$ and δ for the high energy machines. $\Delta\nu_{x \max}$ is nearly independent of δ . Consequently, a machine with high δ can be expected to have a $\Delta\nu_y$ near 0.06 and a $\Delta\nu_x$ from 0.04 to 0.05.

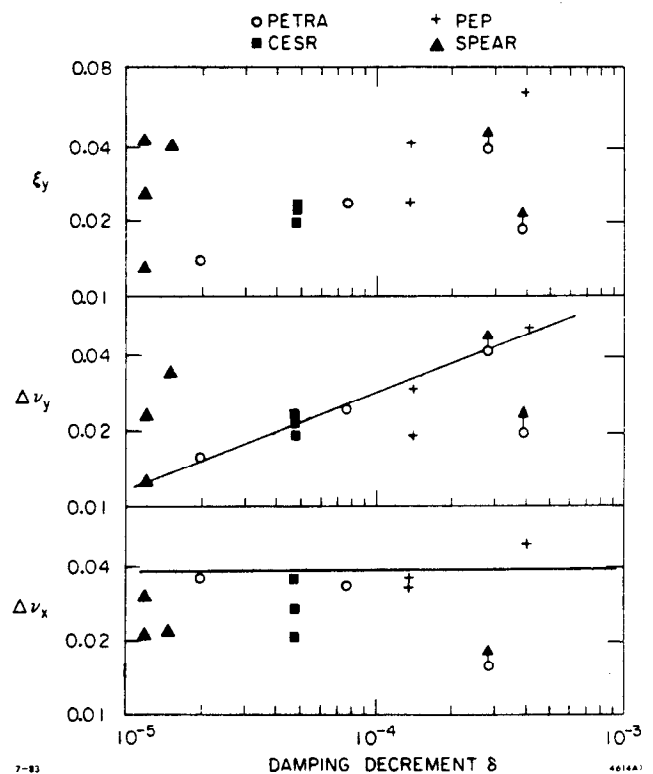


Fig. 4. ξ_y , $\Delta\nu_y$ and $\Delta\nu_x$ versus damping decrement for several machines. Note that $\Delta\nu_y$ is correlated with δ for high energy machines. Data points with arrows are for RF limited conditions.

The choice of tunes and the number of bunches per beam in PEP allows the betatron tune per revolution to be far from an integer to avoid strong synchrotron side bands but the tune per crossing to be near the integer. This allows ξ to be significantly larger than $\Delta\nu$ in both planes. This enhances the peak luminosity. Two consequences are that β_x^* and β_y^* decrease with increasing ξ_x and ξ_y and that a particle ejected from the core of the beam due to the beam-beam interaction experiences lower values of β_x and β_y in the *IR* quadrupoles than does a particle in the core.

Under certain conditions at CESR⁶ and PEP¹², the horizontal tune shift $\Delta\nu_x$ has been observed to limit the current increase after ξ_y has saturated. The cure was to change the tunes or the horizontal crossing parameters. An approximate limit to the horizontal tune shift can be set from Fig. 4.

Luminosity Prediction and Optimization From the observations of the beam-beam interaction at the machines reviewed above, a prescription can be made to describe the current dependence of the luminosity.

Given the desired operating energy and a general geometrical description of a machine, the damping decrement can be calculated and the maximum $\Delta\nu_x$ and $\Delta\nu_y$ determined from Fig. 4. Once the tunes are chosen, $\xi_x \text{ max}$ and $\xi_y \text{ max}$ can be calculated from Eq. (5). Given β_y^* , the half size of the tightest vertical aperture, and the vertical betatron function at that aperture, the maximum value of the vertical beam size at the collision point can be calculated. This beam size must be corrected by the empirical factor of twenty clearance needed at the tightest aperture and by any dynamic beta effects. Finally, once σ_z^* is chosen, the peak current can be calculated from Eq. (2) for $\xi_y \text{ max}$ and the peak luminosity from Eqs. (1) or (4). The resulting value of ξ_x can not exceed $\xi_x \text{ max}$. The luminosity falls linearly with current below the peak value unless the machine conditions are changed or the vertical beam size is reduced to the natural size.

The luminosity must be optimized in three separate ways depending upon whether the current is limited by the beam-beam interaction or not.

Case 1. If the current limit is the beam-beam effect, the peak luminosity is given by combining Eqs. (1) and (2) as described above.

$$L_{\text{max}} \sim \epsilon_y^2 \text{ max } \sigma_z^* \frac{\sigma_y^* \text{ max}}{\beta_y^{*2}} \quad (8)$$

L_{max} is increased (a) by increasing $\xi_y \text{ max}$, (b) by increasing σ_z^* (effectually done at PETRA by changing the RF frequency to increase ϵ_x and at CESR with the aid of nonzero η_x^*), (c) by increasing the tightest vertical aperture to increase $\sigma_y^* \text{ max}$, (d) by reducing β_y at the vertical aperture, and (e) by reducing β_y^* . The effect of reducing β_y^* is subtle. If the aperture limit is in the arcs, β_y at the aperture does not depend on β_y^* , $\sigma_y^* \text{ max} \sim \sqrt{\beta_y^*}$ and $L_{\text{max}} \sim 1/\beta_y^{*3/2}$. This is also the case for "mini" or "micro-beta" projects where β_y at the *IR* quadrupoles remains nearly fixed. However, for those projects β_x^* is typically reduced in a constant ratio to β_y^* , thus $L_{\text{max}} \sim 1/\beta_y^*$ as observed. If the limiting aperture, on the other hand, is in the *IR* quadrupoles, then $\beta_y^* \times \beta_y$ is nearly a constant. Therefore $\sigma_y^* \text{ max} \sim \beta_y^*$, and $L_{\text{max}} \sim \sigma_z^*/\beta_y^*$. If σ_z^* again goes as $\beta_y^{*1/2}$, $L_{\text{max}} \sim 1/\beta_y^{*1/2}$, a slow function.

Case Two. If the current is not limited by the beam-beam interaction but large enough so that ξ_y is still saturated, then the product $\sigma_z^* \sigma_y^*$ can be calculated from Eq. (2) and used in Eq. (1) to determine the luminosity. Trying to reduce σ_z^* to increase the luminosity will fail because σ_y^* will self-adjust to counter balance any change in σ_z^* . Reducing β_y^* will not increase the luminosity, but will expand the beam to fill more of the vertical aperture.

Case Three. If the current is limited but ξ_y is still linear in the current, then from Eq. (1) σ_z^* and σ_y^* should be minimized for maximum luminosity. The methods are to minimize any spurious vertical dispersion, minimize horizontal-vertical coupling, minimize β_y^* consistent with chromaticity corrections and sufficient dynamic aperture, minimize η_x^* , reduce β_x^* , and reduce the horizontal emittance by RF frequency changes.

Core and Tail Suppression The suppression of the growth of the cores of the beams during collisions would allow the tune shift limit to be raised. Studies for the suppression of the cores using tracking programs are in an advanced stage.^{10,19,20} The choice of tunes, tune variations between interaction regions, and spurious dispersion seem to be important parameters.

The suppression of the growth of the non-Gaussian tails of the beams during collisions allows the empirical factor of twenty clearance to be reduced. Tracking programs studying the tails of the beams are now just starting to produce results.¹⁰ Details of the pumping mechanism for elevating particles to large amplitudes need more study. A novel device for increasing the damping for large amplitude particles and defeating the pumping mechanism has been proposed. This device, a quadrupole wiggler,²¹ increases the synchrotron radiation loss per turn for large amplitude particles by exposing them to very strong magnetic fields. The particles near the beam core are unaffected.

Predictions for Future Machines The peak luminosities for e^+e^- collisions in TRISTAN,²² HERA,²³ and LEP²⁴ are predicted using the above prescription. $\xi_x \text{ max}$ and $\xi_y \text{ max}$ come from Fig. 4 assuming $\Delta\nu_{x,y} \text{ max} = \xi_{x,y} \text{ max}$. The values of β_y^* , the size of the smallest aperture, and β_y at that aperture have been reasonably estimated. β_x^* was chosen to make ξ_y and ξ_x limit at the same current. The results are shown in Table 3. The low β_x^* values are needed to make ξ_y saturate. The predicted luminosities are very respectable. However, the required charge per bunch for all machines is about twice that used at PEP. Considering the large transverse impedances and moderate injection energies, there may be difficulties for several of the machines to store sufficient charge to be beam-beam limited.

Table 3. Predictions for Future Machines[†]

Parameter	TRISTAN	HERA	LEP
Energy (GeV)	25	30	51.5
Circ. (km)	3.0	6.3	26.6
$\delta (\times 10^{-4})$	7.7	5.5	4.9
ϵ_x (mm-mrad)	0.11	0.11	0.06
β_y^* (cm)	5	5	10
β_x^* (cm)	22	29	33
$\xi_y \text{ max}$	0.063	0.055	0.053
$\xi_x \text{ max}$	0.05	0.05	0.05
I_{max} (mA)	19	11	2.4
L_{max}	130	79	14
$[\times 10^{30} \text{ cm}^{-2} \text{ sec}^{-1}]$			

[†]Assumptions: Two bunches per beam, a smallest vertical half aperture of 50 mm at β_y of 400 m, and $\eta_x^* = 0$.

Limits to β_y^* Reduction The reduction of β_y^* is very important for increasing the luminosity of a storage ring. Unfortunately, there are two problems which arise at low β_y^* values. First, the chromaticity rapidly increases due to the increasing $\hat{\beta}_y$ in the IR quadrupoles.²⁵ Strong sextupole corrections²⁶ must be made and can limit the dynamic aperture. Moving the IR quadrupoles closer to the interaction point ameliorates this problem. Second, as β_y^* approaches the value of the bunch length σ_z , the luminosity is reduced due to the hour glass effect²⁷ and the tune shift parameter $\xi_{y \max}$ is expected to decrease.¹⁹ Observations on four low β_y^* lattices have been made at CESR.^{7,8} From the prescription for luminosity calculations described above, the ratio of the tail to core enlargement, the saturated value of the vertical tune shift $\xi_{y \max}$, and the quantity $L_{\max} \cdot \beta_y^* / \sigma_z^*$ should be independent of the ratio σ_z / β_y^* for machines with a fixed geometry and a vertical aperture limit near the interaction region. These quantities for the four CESR lattices are plotted versus σ_z / β_y^* in Fig. 5. A factor of three change in the luminosity and two in σ_z^* and β_y^* are concealed in the plots. The three quantities are nearly independent of σ_z / β_y^* at low values. But at the highest points the maximum luminosity drops from that expected, the tune shift limit drops slightly, and the tails grow faster than the core. For the highest σ_z / β_y^* point, the loss in luminosity is attributed to a 12% reduction from the hour glass effect and 30% less current collided due to the additional growth of the tails. From these data, increasing σ_z / β_y^* above 0.7 seems unproductive.

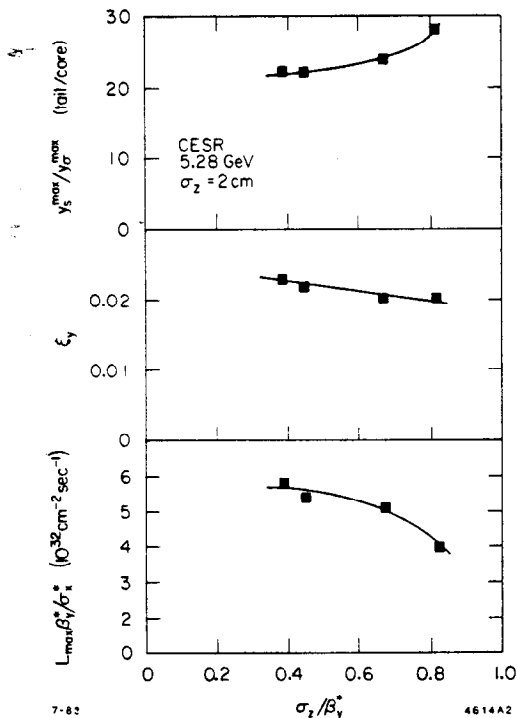


Fig. 5. Low β_y^* measurements at CESR. The lines are to guide the eye.

Conclusion Using observations from several storage rings, a prescription has been formulated which accurately describes the behavior of the luminosity as a function of current. The vertical tune shift is observed to saturate causing the luminosity and

the vertical beam core size to grow linearly with current. The luminosity is limited by non-Gaussian tails which grow with the beam core and ultimately exceed the vertical acceptance. The questions remaining to be answered are

1. what limits the vertical and horizontal tune shift,
2. how does the damping decrement determine $\Delta\nu_{y \max}$,
3. what generates the non-gaussian tails,
4. why do the core and tail grow in proportion, and
5. what in detail happens to the cores and tails of the beams when β_y^* and σ_z are approximately equal?

Furthermore, can the prescription be changed by special conditions or new devices?

Acknowledgements Many thanks go to the courageous operating staffs of SPEAR, CESR, PETRA, and PEP for producing the wealth of data referenced in this paper. Conversations with J. Harris, R. Helm, E. Keil, R. Littauer, B. McDaniel, J. M. Patterson, S. Peggs, A. Piwinski, J. Rees, D. Rice, B. Richter, K. Steffen, R. Talman, M. Tigner, and H. Wiedemann have been very enlightening.

References

1. M. Sands, SLAC-121 (1970).
2. E. Keil, CERN/ISR-TH/74-22 (1974).
3. J. LeDuff, CERN 77-13 (1977) p. 377.
4. H. Wiedemann, SLAC-PUB-2543 (1980).
5. J. Seeman, et al., SLAC-AP-6 (1983).
6. J. Seeman, CLNS 82/531 Cornell (1982).
7. J. Seeman, CBN 82-40 Cornell (1982).
8. Log 43, CESR Op. Group (1982) p. 127.
9. G. Voss, IEEE NS-26, No. 3 (1979) p. 2970.
10. A. Piwinski, Invited paper at 1983 Santa Fe Accelerator Conf.
11. J. Rees, IEEE NS-28, No. 3 (1981) p. 1989.
12. R. Helm, et al., SLAC-PUB-3070 (1983).
13. Log 19, PEP Op. Group (1983) p. 72.
14. D. Degele, et al., DESY M-81/03 (1981).
15. G. Jackson, et al., CBN 83-4, Cornell (1983).
16. H. Wiedemann, SLAC-PUB-2320 (1979).
17. G. Decker, 1983 Santa Fe Accelerator Conf.
18. E. Keil and R. Talman, CERN-ISR-TH/81-33 (1981).
19. S. Myers, CERN-ISR/RF/82-06 (1982).
20. E. Keil, CERN-LEP-TH/83-19 (1983).
21. J. Seeman, CBN 82-32, Cornell (1982).
22. T. Kamei, Y. Kimura, IEEE NS-28, No. 3 (1981) p. 2052.
23. B. Wiik, IEEE NS-28, No. 3, (1981) p. 2020.
24. M. Placidi, LEP Note 394 (1982).
25. K. Steffen, DESY HERA-80/03 (1980).
26. K. Brown, R. Servranckx, this conference.
27. G. Fischer, SLAC-SPEAR-154 (1972).